30% sucrose/PBS, and 15-μm sections hybridized at 52 °C in 50% formamide containing 0.3 M NaCl, 20 mM Tris, pH 7.4, 5 mM EDTA, 10 mM NaH_2PO_4, 1× Denhardt's solution, 10% dextran sulphate, and 0.5 mg ml^{-1} yeast RNA to ^{35}S-labelled RNA probes transcribed from linearized plasmid templates and hydrolysed in alkali to ~300 nucleotide fragments[29]. After washes in 50% formamide and digestion with RNase A, the slides were autoradiographed.

Immunofluorescence. Primary hippocampal cultures were grown on poly-D-lysine-coated glass coverslips for two weeks, fixed in 4% paraformaldehyde/PBS for 20 min, rinsed in PBS, blocked in 0.02% saponin, 2% BSA, 1% fish skin gelatin/PBS (blocking buffer) for 1 h and incubated for 90 min with anti-rVGAT polyclonal rabbit and anti-synaptophysin monoclonal mouse antibodies diluted 1 : 100 in blocking buffer, all at room temperature. The cells were then washed, incubated in secondary anti-rabbit antibody conjugated to fluorescein and anti-mouse antibody conjugated to rhodamine (both Cappel) both diluted 1 : 100, washed, the coverslips mounted on class slides, and viewed under epifluorescence.

Membrane preparation. The rat *unc-47* homologue cDNA subcloned into the plasmid expression vector pcDNA3-Amp (Invitrogen) was introduced into PC12 cells by electroporation[30]. The cells were then selected in 800 μg ml^{-1} G418 (effective) and the resulting clones examined by immunofluorescence[18] using a rabbit polyclonal antibody (R.R., S.M. & R.H.E., manuscript in preparation). Using the two cell clones with the highest level of immunoreactivity, membranes were prepared by first resuspending the washed cells in 0.3 M sucrose, 10 mM HEPES-KOH, pH 7.4 (SH buffer) containing 0.2 mM diisopropylfluorophosphate (DFP), 1 μg ml^{-1} pepstatin, 2 μg ml^{-1} aprotinin, 2 μg ml^{-1} leupeptin, 1 μg ml^{-1} E64 and 1.25 mM MgEGTA. The cells were then disrupted by homogenization at 4 °C through a ball-bearing device at a clearance of 10 μm. The nuclear debris was sedimented at 1,000*g* for 5 min and heavier membranes were eliminated by centrifugation at 27,000*g* for 1 h. The remaining light membrane vesicles were sedimented at 65,000*g* for 1 h and resuspended in SH containing the same protease inhibitors at a final concentration of ~10 μg protein per μl.

Transport assay. To initiate the reaction, 10 μl of membranes was added to 200 μl SH buffer containing 4 mM $MgCl_2$, 4 mM KCl, 4 mM ATP, 40 μM unlabelled GABA and 2 μCi ^{3}H-GABA (NEN). Incubation was performed at 29 °C for varying intervals and the reaction was terminated by rapid filtration (Supor 200, Gelman), followed by immediate washing with 6 ml cold 0.15 M KCl. Background uptake was determined by incubation at 4 °C for 0 min. The bound radioactivity was measured by scintillation counting in 2.5 ml Cytoscint (ICN). To determine K_m, unlabelled GABA was added at a range of concentrations and uptake were measured at 30 s. Nigericin and valinomycin dissolved in ethanol added to final concentrations of 5 μM and 20 μM, respectively. Transport measurements were performed in duplicate and repeated three or more times using at least two different membrane preparations.

Received 18 July; accepted 29 September 1997.

1. Schuldiner, S., Shirvan, A. & Linial, M. Vesicular neurotransmitter transporters: from bacteria to humans. *Physiol. Rev.* **75,** 369–392 (1995).
2. Liu, Y. & Edwards, R. H. The role of vesicular transport proteins in synaptic transmission and neural degeneration. *Annu. Rev. Neurosci.* **20,** 125–156 (1997).
3. McIntire, S., Jorgensen, E. & Horvitz, H. R. Genes required for GABA function in *Caenorhabditis elegans*. *Nature* **364,** 337–341 (1993).
4. Liu, Y. *et al*. A cDNA that supresses MPP+ toxicity encodes a vesicular amine transporter. *Cell* **70,** 539–551 (1992).
5. Erickson, J. D., Eiden, L. E. & Hoffman, B. J. Expression cloning of a reserpine-sensitive vesicular monoamine transporter. *Proc. Natl Acad. Sci. USA* **89,** 10993–10997 (1992).
6. Alfonso, A., Grundahl, K., Duerr, J. S., Han, H.-P. & Rand, J. B. The *Caenorhabditis elegans unc-17* gene: a putative vesicular acetylcholine transporter. *Science* **261,** 617–619 (1993).
7. McIntire, S., Jorgensen, E., Kaplan, J. & Horvitz, H. R. The GABAergic nervous system of *Caenorhabditis elegans*. *Nature* **364,** 334–337 (1993).
8. Wilson, R. *et al*. 2.2 Mb of contiguous nucleotide sequence from chromosome III of *C. elegans*. *Nature* **368,** 32–38 (1994).
9. Brenner, S. The genetics of *Caenorhabditis elegans*. *Genetics* **77,** 71–94 (1974).
10. Chalfie, M., Tu, Y., Euskirchen, G., Ward, W. W. & Prasher, D. C. Green fluorescent protein as a marker for gene expression. *Science* **263,** 802–805 (1994).
11. Clark, S. G., Lu, X. & Horvitz, H. R. The *Caenorhabiditis elegans* locus *lin-15*, a negative regulator of a tyrosine kinase signaling pathway, encodes two different proteins. *Genetics* **137,** 987–997 (1994).
12. Ferguson, E. L. & Horvitz, H. R. Identification and characterization of 22 genes that affect the vulval cell lineages of the nematode *Caenorhabidits elegans*. *Genetics* **110,** 17–72 (1985).
13. Jorgensen, E. M. *et al*. Defective recycling of synaptic vesicles in synaptotagmin mutants of *Caenorhabditis elegans*. *Nature* **378,** 196–199 (1995).
14. Nonet, M. L., Grundahl, K., Meyer, B. J. & Rand, J. B. Synaptic function is impaired but not eliminated in *C. elegans* mutants lacking synaptotagmin. *Cell* **73,** 1291–1306 (1993).
15. Nonet, M. L. *et al*. Functional synapses are partially depleted of vesicles in *C. elegans rab-3* mutants. *J. Neurosci.* (in the press).
16. Hall, D. H. & Hedgecock, E. M. Kinesin-related gene *unc-104* is required for axonal transport of synaptic vesicles in *C. elegans*. *Cell* **65,** 837–847 (1991).
17. Thomas-Reetz, A. *et al*. γ-aminobutyric acid transporter driven by a proton pump is present in synaptic-like microvesicles of pancreatic B cells. *Proc. Natl Acad. Sci. USA* **90,** 5317–5321 (1993).
18. Liu, Y. *et al*. Preferential localization of a vesicular monoamine transporter to dense core vesicle in PC12 cells. *J. Cell Biol.* **127,** 1419–1433 (1994).
19. Varoqui, H. & Erickson, J. D. Active transport of acetylcholine by the human vesicular acetylcholine transporter. *J. Biol. Chem.* **271,** 27229–27232 (1996).
20. Fykse, E. M. & Fonnum, F. Uptake of γ-aminobutyric acid by a synaptic vesicle fraction isolated from rat brain. *J. Neurochem.* **50,** 1237–1242 (1988).
21. Hell, J. W., Maycox, P. R., Stadler, H. & Jahn, R. Uptake of GABA by rat brain synaptic vesicles isolated by a new procedure. *EMBO J.* **7,** 3023–3029 (1988).
22. Kish, P. E., Fischer-Bovenkerk, C. & Ueda, T. Active transport of γ-aminobutyric acid and glycine into synaptic vesicles. *Proc. Natl Acad. Sci. USA* **86,** 3877–3881 (1989).
23. Burger, P. M. *et al*. GABA and glycine in synaptic vesicles: storage and transport characteristics. *Neuron* **7,** 287–293 (1991).
24. Naito, S. & Ueda, T. Adenosine triphosphate-dependent uptake of glutamate into protein I-associated synaptic vesicles. *J. Biol. Chem.* **258,** 696–699 (1983).
25. Maycox, P. R., Deckwerth, T., Hell, J. W. & John, R. Glutamate uptake by brain synaptic vesicles. Energy dependence of transport and functional reconstitution in proteoliposomes. *J. Biol. Chem.* **263,** 15423–15428 (1988).
26. Carlson, M. D., Kish, P. E. & Ueda, T. Glutamate uptake into synaptic vesicles: competitive inhibition by bromocriptine. *J. Neurochem.* **53,** 1889–1894 (1989).
27. Christensen, H., Fykse, E. M. & Fonnum, F. Inhibition of γ-aminobutyrate and glycine uptake into synaptic vesicles. *Eur. J. Pharmacol.* **207,** 73–79 (1991).
28. Fischer, W. N., Kwart, M., Hummel, S. & Frommer, W. B. Substrate specificity and expression of profile of amino acid transporters (AAPs) in *Arabidopsis*. *J. Biol. Chem.* **270,** 16315–16320 (1995).
29. Sassoon, D. & Rosenthal, N. in *Guide to Techniques in Mouse Development* (eds Wassarman, P. M. & DePamphilis, M. L.) 384–404 (Academic, San Diego, 1993).
30. Grote, E., Hao, J. C., Bennett, M. K. & Kelly, R. B. A targeting signal in VAMP regulating transport ot synaptic vesicles. *Cell* **81,** 581–589 (1995).

Acknowledgements. We thank B. Westlund for unpublished *unc-47* map data; E. King for help with the confocal microscope; H. Rausch and K. Knobel for integrating the *unc-47*::GFP transcriptional fusion construct; Y. Jin for the *n2476* allele; D. P. Morse and B. Bamber for the gift of RNA and cDNA; R. Barstead and P. Okkema for the *C. elegans* cDNA libraries; J. Boulter and D. Julius for the mammalian cDNA libraries; D. Rice and D. Eisenberg for the analysis of hydrophobic moment; A. Tobin and S. Baekkeskov for the GAD-67 cDNA; Y. Liu and P. Tan for assistance in the isolation of PC12 cell clones and the preparation of membranes; J. Hell and P. Finn for suggestions about the measurement of transport activity; S. Craven and D. Bredt for assistance with the primary hippocampal cultures; and M. Horner, E. Kofoid, C. Bargmann and members of the Edwards and Jorgensen laboratories for discussions. This work was supported by the Gallo Center (S.L.M.), the Giannini Foundation (R.J.R.), an NIH Developmental Biology training grant (K.S.), the Klingenstein Foundation (E.M.J.), NINDS (S.L.M., R.H.E., E.M.J.) and NIMH (R.H.E.).

Correspondence and requests for materials should be addressed to R.H.E. (e-mail: edwards@itsa.ucsf.edu) or E.M.J. (e-mail: jorgensen@bioscience.biology.utah.edu).

Activation of the transcription factor Gli1 and the Sonic hedgehog signalling pathway in skin tumours

N. Dahmane*, J. Lee*, P. Robins†, P. Heller† & A. Ruiz i Altaba*

** The Skirball Institute, Developmental Genetics Program and Department of Cell Biology, and † Department of Dermatology, New York University Medical Center, 540 First Avenue, New York, New York 10016, USA*

Sporadic basal cell carcinoma (BCC) is the most common type of malignant cancer in fair-skinned adults. Familial BCCs and a fraction of sporadic BCCs have lost the function of Patched (Ptc), a Sonic hedgehog (Shh) receptor[1–3] that acts negatively on this signalling pathway. Overexpression of Shh can induce BCCs in mice[4]. Here we show that ectopic expression of the zinc-finger transcription factor Gli1 in the embryonic frog epidermis results in the development of tumours that express endogenous *Gli1*. We also show that *Shh* and the *Gli* genes are normally expressed in hair follicles, and that human sporadic BCCs consistently express *Gli1* but not *Shh* or *Gli3*. Because Gli1, but not Gli3, acts as a target and mediator of Shh signalling[5], our results suggest that expression of Gli1 in basal cells induces BCC formation. Moreover, loss of Ptc or overexpression of Shh cannot be the sole causes of Gli1 induction and sporadic BCC formation, as they do not occur consistently. Thus any mutations leading to the expression of Gli1 in basal cells are predicted to induce BCC formation.

Gli1, which was originally isolated as an amplified gene in a glioma[6], is a member of a multigene family[7–9] and can transform

fibroblasts in cooperation with adenovirus E1A[10]. Ectopic expression of Gli1 in frog embryos activates Shh target genes, including that encoding HNF-3β, both in neural and epidermal non-neural ectoderm[5,11], showing that epidermal cells can respond to Shh signalling. Frog embryos injected with plasmids driving the expression of frog *Gli1* developed abnormal growths, or tumours, in the otherwise normal, smooth tadpole epidermis (78%, $n = 25$; Fig. 1a). The tumours were independent of HNF-3β expression, as only a fraction contained cells expressing HNF-3β (30%, $n = 27$). Because the plasmid DNA was targeted to the animal-most region of the two-cell embryo, only ectodermal derivatives inherit plasmids, indicating that the growths of focal epidermal hyperplasia (the tumours) observed are caused by expression of Gli1 in the epidermis. Indeed, detection of epitope-tagged Gli1 in injected embryos showed exclusive expression in the ectoderm[5] (not shown). Histological sections of 1-week-old (stage ~45) injected tadpoles revealed tumours in the epidermis, sometimes consisting of densely packed cells (Fig. 1f). These cells were clearly distinct from all normal tissues (Fig. 1e) and did not express the cement-gland marker *XAG-1* (ref. 12) ($n = 10$; not shown). Taken together, these results show that transient epidermal expression of Gli1 leads to tumour formation *in vivo*.

To determine whether tumours formed from cells inheriting injected *Gli1*, embryos were co-injected with frog *Gli1* RNA and *lacZ* RNA as tracer. Injected tadpoles showed prominent tumours of the skin (80%, $n = 12$) formed from the superposition of epidermal cells that inherited *Gli1*, as these invariably expressed β-galactosidase (Fig. 1b–d). Labelled epidermal cells located inside the tumours were distinct from the underlying lateral-plate mesoderm, which was always unlabelled. The uninjected side displayed typical smooth embryonic epidermis (Fig. 1c, right) and injection of *lacZ* alone had no effect. Because not all epidermal cells inheriting *Gli1* RNA become tumorigenic, there could be a requirement for a certain level of Gli1 to initiate tumour formation. The effects of Gli1 are specific, as injection of plasmids driving the expression of human *Gli3* (ref. 7) had no effect[5] ($n = 45$; not shown). Inappropriate expression of Gli1 therefore leads to tumour formation, although it is not clear if this represents epidermal neoplastic transformation.

The finding of mutated *Ptc* alleles in familial and some sporadic BCCs[1–3] together with the development of skin tumours in tadpoles overexpressing Gli1 raised the possibility that Gli1 could be expressed in and underlie the development of sporadic adult basal cell cancer. Sections of freshly excised human BCCs were analysed by *in situ* hybridization. All but one of the samples examined showed unambiguous expression of *Gli1*, although the level of expression varied (46 of 47; Table 1, Fig. 2). The variability observed in *Gli1* RNA expression could be due to inherent differences in the tumours or to differences in the preservation of the excised material. No correlation was detected between the level of *Gli1* expression and the site or the aggressiveness of the tumour. In contrast to the consistent expression of *Gli1*, only 76% (23 of 30; Table 1) of the cases displayed unequivocal expression of *Gli3* (Fig. 2k), which is often coexpressed with *Gli1* (refs 5, 9, 13, 14). Analysis of ten cases of squamous cell carcinoma (SCC) *in situ* showed *Gli* gene expression to be absent (Table 1, Fig. 2s, t). Control hybridizations with sense RNA probes showed no signal (Table 1, Fig. 2l).

Tumour nodules infiltrating the dermis showed the highest levels of *Gli1* expression (Fig. 2a–f, i, j, n), and here it was often concentrated in the periphery (Fig. 2f, j), where most proliferating cells appear to be located[15]. In tumorigenic regions, the basal layer of the epidermis also displayed high levels of *Gli1* expression (Fig. 2c–e). The pattern of expression of *Gli3* was distinct from that of *Gli1* but was also detected primarily in the periphery of tumour nodules (Fig. 2k). *Gli* gene expression was not detected in the interfollicular epidermis or the dermis in normal regions distal from the tumour (Fig. 2q, r), although *Gli1* mRNA was detected in histologically normal basal cells immediately surrounding the tumour site (Fig. 2a, b, right). Cells of the sebaceous glands, dermis and blood vessels were negative. Single cells surrounding the main BCC tumour masses were rarely positive for *Gli1* (3 of 47) or *Gli3* expression (1 of 30; Fig. 2j, k), and could represent early invading tumour cells that are histologically unrecognizable. Alternatively, these single cells may be non-BCC cells that express *Gli1* in response to a secreted tumour-derived factor.

Expression of Gli1 was also analysed by immunocytochemistry with an affinity-purified anti-human Gli1 polyclonal antibody[5]. All samples showed specific Gli1 expression (6 of 6; Table 1; Fig. 2u–w). Control antibody labelling with an anti-HNF-3β polyclonal antibody[11,16] showed no specific labelling (Table 1 and data not shown). In BCCs, Gli1 protein was detected in the cytoplasm (Fig. 2u, w), consistent with the prevalent cytoplasmic localization of frog Gli1 (ref. 5). This is also consistent with an association of Gli proteins with the cytoskeleton[17], but contrasts with the nuclear localization of Gli1 in COS cells transfected with the glioma-derived cDNA[5] (Fig. 2x) and in a glioma line showing a 75-fold overexpression of *Gli1* (D259MG[6,18]). The glioma cDNA[6] thus appears to encode a mutated protein that escapes cytoplasmic retention.

The possibility that Gli1 could activate components of the Shh signal-transduction pathway in sporadic BCCs, including endogenous human *Shh* itself[19,20], was suggested by the regulatory loop

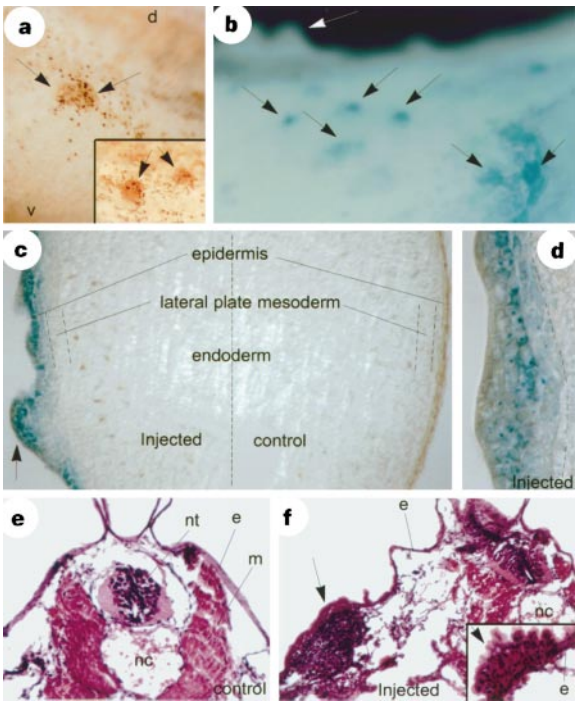

Figure 1 Ectopic expression of Gli1 in frog embryos leads to the formation of epidermal tumours. **a**, **b**, Whole-mount view of the flank of injected tadpoles (stages ~32–34) showing epidermal tumours (arrows) and cells expressing HNF-3β (brown). The embryo in **b** was co-injected with *Gli* synthetic RNA and *lacZ* RNA as tracer. β-Gal activity is shown in blue; d, dorsal; v, ventral. **c**, **d**, Histological cross-sections through the trunk of embryos unilaterally injected with Gli1. The affected side is blue (arrow, left in **c**). **d**, Detail of a tumour similar to that shown in **c** in which β-gal activity is detected as small cytoplasmic inclusions. The boundaries between the epidermis and the underlying lateral plate mesoderm and between this and the endoderm are denoted by broken lines. **e**, **f**, Histological sections stained with haematoxylin and eosin through the trunk of control (**e**) and Gli1-injected (**f**) stage ~45 tadpoles. An epidermal tumour is detected in the flank (arrow in **f**). The inset in **f** shows an outwardly growing epidermal tumour (arrow); e, epidermis; m, muscle; nc, notochord; nt, neural tube. Dorsal side is up in all cases. In **a** and **b**, anterior is to the left.

defined in the Shh signalling pathway in which Shh signalling triggers a cascade of events leading to the activation of *Gli1*, which in turn may activate the transcription of Shh target genes including *Shh* and *Ptc*. By *in situ* hybridization, 44% (15 of 34) of BCCs were positive for *Shh*, with expression localized to the tumour masses that also expressed *Gli1* (Fig. 2o, Table 1). Analysis of nine SCCs *in situ* showed no *Shh* expression (Table 1). Sense *Shh* RNA probes showed no specific signal (Table 1). Reverse transcription–polymerase chain reaction (RT–PCR) analyses revealed *Shh* expression in two cases of BCC, whereas this was below the level of detection in three BCCs and one SCC *in situ*. All these samples showed low levels of *Gli3* expression, and all five BCCs, but not the SCC, showed elevated levels of *Gli1* and *Ptc* mRNAs. Expression of the ribosomal gene *S17* was monitored as a control (not shown). The lower frequency of *Shh* (17 or 37 cases overall) compared with *Gli1* expression (49 of 50 cases overall) in BCCs, together with the inability of injected Shh to initiate epidermal tumour formation in frog embryos[11], suggests that Shh is unlikely to be the only cause of *Gli1* expression in BCCs, and that *Shh* may not be regulated solely by Gli1. In contrast, Ptc was expressed in all BCCs examined[3] (16 of 16; Fig. 2p, Table 1 and not shown), and was coincident with *Gli1* and *Shh* (Fig. 2m–o), consistent with *Ptc* being a target of Gli1.

Tadpole tumours induced by Gli1 could be the equivalent of human BCCs. However, morphological analyses, the main criteria of dermatopathologists, cannot be applied to the tadpole tumours as early tadpoles do not have dermis. Our molecular analysis of BCCs provides an alternative test for the BCC-like nature of tadpole tumours, as endogenous *Gli1* is expressed consistently in the human tumours (Table 1, Fig. 2). Injection of human Gli1, which we have previously shown has a similar activity to frog Gli1 (ref. 5), resulted in the formation of epidermal tumours (79%, $n = 24$), and all tumours displayed expression of the endogenous frog *Gli1* gene (Fig. 3a–c). Endogenous *Gli1* expression was not detected in non-tumorigenic regions of the epidermis in injected embryos or control siblings (Fig. 3a). In contrast, only a small fraction (12–23%) of embryos injected with *Gli1* mRNA or pDNA showed ectopic *Shh* expression, mostly in the non-tumorigenic epidermis of injected tadpoles (3 of 25 for RNA, Fig. 3e; and 7 of 30 for pDNA) and early neurulae[11], not observed in controls (Fig. 3d). The low incidence of *Shh* expression and the consistent expression of *Gli1* in tadpole epidermal tumours parallels that found in BCCs and points to their having a BCC-like nature.

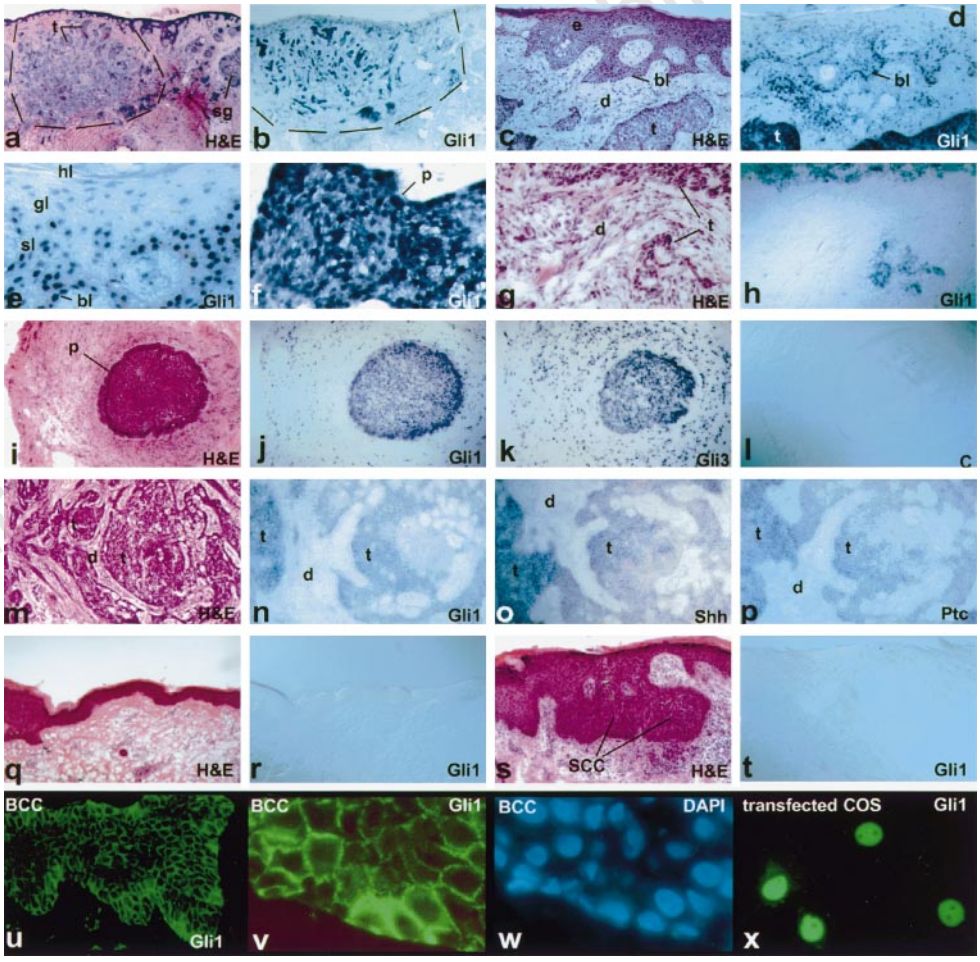

Figure 2 Gene expression in basal cell carcinomas and cell lines. **a**–**p**, Sections of BCC excisions showing the distribution of tumour masses as seen by histological staining (**a**, **c**, **g**, **i**, **m**), *Gli1* mRNA (**b**, **d**, **e**, **f**, **h**, **j**, **n**), *Gli3* mRNA (**k**), *Shh* mRNA (**o**) or *Ptc* mRNA (**p**). As a control, absence of label is seen after hybridization with a *Gli1* sense probe (**l**). Matched samples from the same specimens are shown in **a** and **b**, **c** and **d**, **g** and **h**, **i** to **l**, and **m** to **p**, **e**, **f**, Details of the specimen shown in **a**–**d**, respectively. **q**, **r**, Sections of normal skin distal from tumorigenic regions in a BCC excision showing the absence of *Gli1* expression. **s**, **t**, Sections of an excised sample of squamous cell carcinoma (SCC) *in situ* showing the absence of *Gli1* expression. **u**–**x**, Labelling of excised BCC sections with affinity-purified anti-human Gli1 antibodies (**u**, **v**, **x**) or with the DNA-binding dye DAPI showing the position of nuclei (blue in **w**). **x**, Expression of nuclear Gli1 protein in COS-7 cells transfected with plasmids driving the expression of the human glioma *Gli1* cDNA. H&E, haematoxylin and eosin stain; bl, basal layer; d, dermis; e, epidermis; gl, granular layer; hl, horny layer; p, pallisade in the periphery of the tumour nodule; sl, spiny layer; t, tumour. In all cases the skin surface is up except in **i**–**l** in which it is to the left. **a**–**f**, case no. 5; **g**, **h**, case no. 7; **i**–**l**, case no. 12; **m**–**p**, case no. 61; **q**, **r**, a normal skin region of case no. 18; **s**, **t**, case no. 15; all as listed in Table 1.

Table 1 Gene expression in human skin tumours

Case	type	location	Gli1 ab	HNF-3β Ab	Gli1-as	Gil1-s	Gli3-as	Gli3-s	Shh-as	Shh-s	Ptc-as	H&E
1	BCC	auricular	+									+
2	BCC	nasolabial fold	+	–								+
3	BCC	temple	+	–								+
4	BCC	forehead	+									+
5	BCC	post-auricular			++							+
6	BCC	inner canthus	+	–	++							+
7	BCC	post-auricular	+	–	++	–						+
8	BCC	nasolabial fold			++							+
9	BCC	post-auricular			++							+
10	BCC	canthus			+/–	–	+/–					+
11	BCC	canthus			+	–	+					+
12	BCC	back			++	–	++	–				+
13	BCC	nasal rim			++	–		–				+
14	BCC	nasal rim			++	–	–	–				+
17	BCC	nasal rim			+/–	–	–	–				+
18	BCC	nasal rim			++	–	–	–				+
24	BCC	nose			+		–		+			+
26	BCC	periareolar			++		+		++	–		+
27	BCC	eyelid			+		–		–	–		+
28	BCC	nose			+		+/–	–	–			+
29	BCC	temple			+		+		+	–		+
30	BCC	midback			++		+		+	–		+
32	BCC	lat. forehead			+		–		–			+
33	BCC	eyebrow			+		+		+			+
34	BCC	nosetip			+		+		–			+
37	BCC	lat. upper cheek			+/–		+/–		+/–			+
39	BCC	upper lip			+		+		+/–			+
41	BCC	malar ocular			++		++		+/–			+
42	BCC	malar ocular			++		+		–			+
43	BCC	temple			++		+		–			+
44	BCC	nose			+		+		–			+
45	BCC	cheek			++		+		+			+
46	BCC	nostril			++		++		–			+
47	BCC	zygoma			++		+		–			+
48	BCC	upper eyelid			+		++		+			+
51	BCC	glabella			++		+		+			+
52	BCC	nose			+		++		–			+
53	BCC	nose			+		+/–		–			+
54	BCC	ear			++		+/–		+/–			+
57	BCC	clavicle			+		–		–			+
59	BCC	nose			++				+	–	++	+
61	BCC	nose			++				++	–	+	+
63	BCC	nose			+						++	+
64	BCC	forehead			+/–				–	–	++	+
66	BCC	temple			+				–	–	+	+
67	BCC	forehead			+				+	–	++	+
69	BCC	forehead			++				–	–	++	+
70	BCC	scalp			++				–	–	++	+
71	BCC	eye			+				–	–	+	+
72	BCC	nose			++				–	–	++	+
74	BCC	temple			+				–	–	+	+
15	SCC	upper back			–	–	–	–				+
23	SCC	preauricular			–		–		–	–		+
25	SCC	eyelid			–		–		–	–		+
31	SCC	elbow			–		–		–			+
35	SCC	cheek			–		–		–			+
40	SCC	cheek			–		–		–			+
49	SCC	cheek			–		–		–	–		+
55	SCC	hand			–		+/–		–	–		+
56	SCC	neck			–		–		–	–		+
58	SCC	bridge nose			–		–		–	–		+

The case number, type of tumour (BCC or SCC *in situ*) and location of the tumour is given on the left. The presence (+) or absence (–) of gene expression is indicated, with strong expression indicated by ++. A section of each excision was also stained with haematoxylin and eosin (H&E) for histological examination and confirmation of the presence of tumour. Case no. 10 was ambiguous and was counted as negative for *Gli1* expression. Abbreviations: as, antisense RNA probe; s, sense RNA probe; Ab, antibody; lat., lateral.

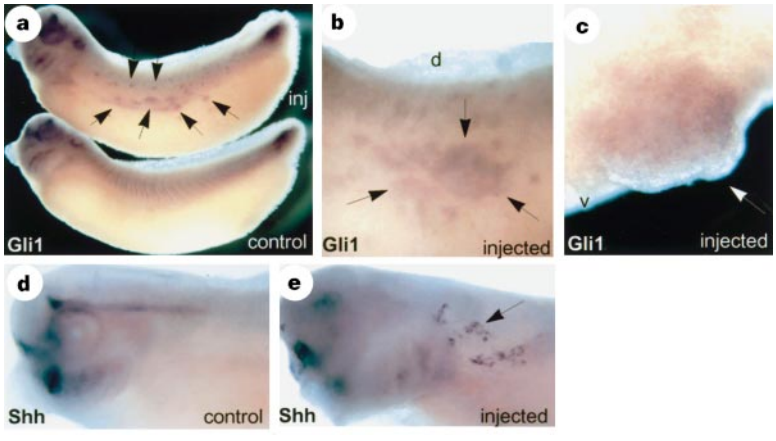

Figure 3 Expression of endogenous *Gli1* and *Shh* in Gli1-induced tadpole tumours. Frog tadpoles (stages 34–36) injected with human *Gli1* plasmids (**a**–**c**) or synthetic frog *Gli1* RNA (**e**), but not control embryos (**a** bottom **d**), show ectopic expression of endogenous *Gli1* (arrows in **a** top, **b**, **c**) or *Shh* (arrow in **e**). Human and frog *Gli1* do not cross-hybridize *in situ* hybridization. Gli1 is normally expressed in several tissues including the neural tube but not the early epidermis[11]. *Shh* is normally expressed in the nervous system and head structures including the branchial arches[5]. Anterior is to the left and dorsal side is up. Embryos were not cleared.

Interfollicular human basal cells and the early tadpole epidermis do not normally express *Gli1* genes, and the reason why the epidermis is responsive to Shh and Gli1 is not clear. However, we detected expression of *Gli1* and *Shh* in human hair follicles, and *Shh*, *Gli1*, *Gli2* and *Gli3* were also expressed in mouse hair follicles[14,21,22] during the growing phases with highest expression of *Shh* and *Gli1* in matrix keratinocytes of the bulb (not shown). This indicates that normal epidermal development involves the selective activation of the Shh signalling pathway during follicular formation and provides a context for the ability of embryonic and non-follicular-basal epidermal cells to respond to overexpression of Gli1.

Gli1 has been found to be amplified only in a small number of gliomas and other tumours[6,24,25]. The high incidence of *Gli1* expression in BCCs contrasts with the relatively infrequent occurrence of other oncogenes, such as mutated *ras* alleles[23]. Because hair follicles normally activate the Shh signalling pathway during growth, BCCs could derive from the neoplastic transformation of these cells. Indeed, BCCs show traits of follicular differentiation[26], including the expression of *Gli3*. It is possible, however, that BCCs derive from non-follicular basal cells which express Gli1 ectopically. In this case, the normal interaction taking place between the dermal papilla and the hair bulb could be activated inappropriately in non-follicular basal cells, resulting in the activation of the Shh signalling pathway and formation of BCCs. We propose that any mutations that activate the Shh signalling pathway will lead to ectopic Gli1 expression and BCC formation. In familial BCCs showing loss of Ptc function[1,2], we predict that Gli1 will be ectopically expressed. However, mutations in Ptc cannot account entirely for Gli1 activation. We found that *Gli1* and *Ptc* are consistently expressed in sporadic BCCs, whereas in other studies only a fraction of sporadic BCCs showed an altered *Ptc* allele[2,3]. Because there may be a regulatory loop in the Shh signalling pathway, Gli1 expression would appear to be both a cause and an effect of BCC development.

Ectopic expression of Shh in basal cells of transgenic mice has recently been shown to result in the development of BCC-like tumours[4]. However, the inability of Shh to induce tumour formation in the tadpole epidermis and its inconsistent expression in BCCs and tadpole tumours raise the possibility that normally there may be restrictions to the induction and action of Shh in epidermis similar to those present in the neural plate[11]. Such restrictions could prevent BCC formation adjacent to follicle cells expressing Shh during normal hair growth and after plucking, and the uncontrolled spread of BCCs throughout the surrounding tissue when the tumours induce Shh. Independent of whether Shh can initiate BCC formation, its expression in BCCs suggests a mode of autocrine tumour maintenance as secreted Shh from the tumour cells could activate its signalling pathway, leading to new expression of *Gli1*. Activation of autocrine Shh signalling could underlie the formation of persistent epidermal tumours in embryos that transiently expressed Gli1 through microinjection. However, transcription of endogenous *Gli1* but not *Shh* was always detected in Gli1-induced tumours and BCCs, suggesting that a Gli1 regulatory loop operating downstream of Shh is functional.

The recurrence of BCCs at sites adjacent to previous tumours could result from the observed ectopic expression of Gli1 in basal cells in a wide region extending beyond the neoplastic sites. This raises the possibility that Gli1 expression in basal cells is an early event and could be used as a diagnostic tool. Finally, therapeutic agents for BCCs are likely to include inhibitors of the Shh signalling pathway and Gli1 function. □

Methods

Embryos and microinjection. *Xenopus laevis* embryos were obtained and manipulated by standard procedures[27]. Microinjections were performed into the animal-most region of one cell at the two-cell stage to bias the distribution of the injected plasmids or RNAs to the ectoderm and to have half of the embryo as an undisturbed internal control. Plasmid DNA (200 pg) or synthetic RNAs (2 ng) made by *in vitro* transcription were delivered by microinjection. Frog *Gli1*, human *Gli1* and *Gli3* plasmids were as described[5].

***In situ* hybridization, immunocytochemistry, histology and cell lines.** Frog embryos were processed for *in situ* hybridization with digoxigenin-labelled RNA probes[28]. Frog *Gli1* and *Shh* plasmids to make sense or antisense RNA probes were as described[5]. Frozen cryostat sections of tumour specimens excised by the Mohs technique (by P.R.) were processed by *in situ* hybridization with digoxigenin-labelled RNA probes[29]. Plasmids with human *Gli1* and *Gli3* cDNAs[6,7] and mouse *Shh* and *Gli1–3* cDNAs used to make sense and anti-sense RNA probes were as described[5]. The human *Shh* probes were made from a plasmid subclone of a 409-base pair RT–PCR product or from a human cDNA[19]. Immunocytochemistry with anti-human Gli1 affinity-purified polyclonal antibodies[5], anti-frog HNF-3β or anti-rat HNF-3β polyclonal antibodies[11,16] were performed in whole-mount labelling or in 5–15 μm cryostat sections. Nuclei were visualized by staining with the DNA-binding dye DAPI after antibody incubations. Histological sections of injected tadpoles were obtained by cutting paraplast-embedded samples in a microtome[5]. These sections and one section of each tumour sample were also stained with haematoxylin and eosin for histological and pathological examination (by P.H.). β-Galactosidase activity was revealed by the X-gal reaction. COS-7 cells were obtained from ATCC and cultured under the specified conditions. Transfections were performed with lipofectamine (Gibco-BRL) as specified by the manufacturer. Cells were assayed 24–48 h after transfection.

RNA isolation and RT–PCR. RNA from frozen excisions was extracted by the guanidinium isothiocyanate, acid phenol method. cDNA was made with random hexamers and BRL Superscript reverse transcriptase. PCR was performed at 57 °C for 40 cycles with the following primers to human *Gli1*: Gli1-U, CAGAGAATGGAGCATCCTCC; and Gli1-D, TTCTGGCTCTTCCT GTAGCC, yielding a 412-bp product. Human *Gli3*: Gli3-U, GCAGCCACAG AATGTCC; and Gli3-D, AGGGATATCCAATCGAGGAATCG, yielding a 293-bp product. Human *Shh*: Shh-U2, GAAGATCTCCAGAAACTCC; and Shh-D, TCGTAGTGCAGAGACTCC, yielding a 233-bp product. Mouse *S17*, which works well with human cDNA: S17-U, GCTATGTCACGCATCTGATG; and S17-D, CCTCAATGATCTCCTGATC, yielding a 137-bp product. Human *Ptc*: Ptc-U, GAATCCAGGCATCACCCACC; and Ptc-D, CCACGTCCTGCAGCTC AATG, yielding a 490-bp product. The RT–PCR *shh* clone used to make RNA probes derived from a reaction using Shh-U1, AGATGTCTGCTGCTAGTCC, and Shh-D. *Shh* RNA probes were also made from a large human cDNA[19].

Received 26 June; accepted 5 August 1997.

1. Hahn, H. *et al.* Mutations of the human homolog of *Drosophila patched* in the nevoid basal cell carcinoma syndrome. *Cell* **85,** 841–851 (1996).
2. Johnson, R. L. *et al.* Human homolog of patched, a candidate gene for the basal cell nevus syndrome. *Science* **272,** 1668–1671 (1996).
3. Gailani, M. R. *et al.* The role of the human homologue of the *Drosophila* patched in sporadic basal cell carcinomas. *Nature Genet.* **14,** 78–81 (1996).
4. Oro, A. E. *et al.* Basal cell carcinomas in mice overexpressing Sonic hedgehog. *Science* **276,** 817–821 (1997).
5. Lee, J., Platt, K. A., Censullo, P. & Ruiz i Altaba, A. *Gli1* is a target of Sonic hedgehog that induces ventral neural tube development. *Development* **124,** 2537–2552 (1997).
6. Kinzler, K. W. *et al.* Identification of an amplified, highly expressed gene in a human glioma. *Science* **236,** 70–73 (1987).
7. Ruppert, J. M., Vogelstein, B., Arheden, K. & Kinzler, K. W. GLI3 encodes a 190 kilodalton protein with multiple regions of GLI similarity. *Mol. Cell. Biol.* **10,** 5048–5415 (1990).
8. Walterhouse, D. *et al.* Gli, a zinc finger transcription factor and oncogene, is expressed during normal mouse development. *Dev. Dyn.* **196,** 91–102 (1993).
9. Hui, C.-C., Slusarski, D., Platt, K. A., Holmgren, R. & Joyner, A. L. Expression of three mouse homologs of the *Drosophila* segment polarity gene cubitus interruptus, Gli, Gli2 and Gli3 in ectoderm and mesoderm-derived tissues suggests multiple roles during postimplantation development. *Dev. Biol.* **162,** 402–413 (1994).
10. Ruppert, J. M., Vogelstein, B. & Kinzler, K. W. The zinc finger protein GLI transforms primary cells in cooperation with adenovirus E1A. *Mol. Cell. Biol.* **11,** 1724–1728 (1991).
11. Ruiz i Altaba, A., Jessell, T. M. & Roelink, H. Restrictions to floor plate induction by *hedgehog* and winged helix genes in the neural tube of frog embryos. *Mol. Cell. Neurosci.* **6,** 106–121 (1995).
12. Sive, H. L., Hattori, K. & Weintraub, H. Progressive determination during formation of the anteroposterior axis in *Xenopus laevis*. *Cell* **58,** 171–180 (1989).
13. Marigo, V., Johnson, R. L., Vortkamp, A. & Tabin, C. J. Sonic hedgehog differentially regulates expression of Gli and Gli3 during limb development. *Dev. Biol.* **180,** 273–283 (1996).
14. Platt, K. A., Michaud, J. & Joyner, A. L. Expression of the mouse Gli and Ptc genes is adjacent to embryonic sources of hedgehog signals suggesting a conservation of pathways between flies and mice. *Mech. Dev.* **62,** 121–135 (1997).
15. Grimwood, R. E., Ferris, C. F., Mercill, D. B. & Hugg, J. C. Proliferating cells of human basal cell carcinoma are located on the periphery of tumor nodules. *J. Invest. Dermatol.* **86,** 191–194 (1986).
16. Ruiz i Altaba, A., Placzek, M., Baldassare, M., Dodd, J. & Jessell, T. M. Early stages of notochord and floor plate development in the chick embryo defined by normal and induced expression of HNF-3β. *Dev. Biol.* **1270,** 299–313 (1995).
17. Ruiz i Altaba, A. Catching a Gli-mpse of hedgehog. *Cell* **90,** 193–196 (1997).

18. Kinzler, K. W. & Vogelstein, B. The *GLI* gene encodes a nuclear protein which binds specific sequences in the human genome. *Mol. Cell. Biol.* **10,** 634–642 (1990).
19. Belloni, E. *et al.* Identification of Sonic hedgehog as a candidate gene responsible for holoprosencephaly. *Nature Genet.* **14,** 353–356 (1996).
20. Roessler, E. *et al.* Mutations in the human Sonic hedgehog gene cause holoprosencephaly. *Nature Genet.* **14,** 357–360 (1996).
21. Iseki, S. *et al.* Sonic hedgehog is expressed in epithelial cells during development of whisker, hair, and tooth. *Biochem. Biophys. Res. Commun.* **218,** 688–693 (1996).
22. Bitgood, M. J. & McMahon, A. P. Hedgehog and Bmp genes are coexpressed at many diverse sites of cell-cell interaction in the mouse embryo. *Dev. Biol.* **172,** 126–138 (1996).
23. van der Schroeff, J. G., Evers, L. M., Boot, A. J. M. & Box, J. L. Ras oncogene mutations in basal cell carcinomas and squamous cell carcinomas of human skin. *J. Invest. Dermatol.* **94,** 423–425 (1990).
24. Roberts, W. M., Douglass, E. C., Peiper, S. C., Houghton, P. J. & Look, A. T. Amplification of the *gli* gene in childhood sarcomas. *Cancer Res.* **49,** 5407–5413 (1989).
25. Xiao, H., Goldthwait, D. A. & Mapstone, T. A search for Gli expression in tumors of the central nervous system. *Pediatr. Neurosurg.* **20,** 178–182 (1994).
26. Ackerman, A. B., DeViragh, P. A. & Chongchitnant, N. *Neoplasms with Follicular Differentiation* (Lea and Febinger, Philadelphia, 1993).
27. Ruiz i Altaba, A. in *Essential Developmental Biology—A Practical Approach* (eds Stern, C. & Holland, P. W. H.) (IRL, Oxford, 1993).
28. Harland, R. M. In situ hybridization: an improved whole mount method for *Xenopus* embryos. *Methods Enzymol.* **36,** 675–685 (1991).
29. Scharen-Wiemers, N. & Gerlin-Moser, A. A single protocol to detect transcripts of various types and expression levels in neural tissue and cultures cells: in situ hybridization using digoxygenin-labeled cRNA probes. *Histochemistry* **100,** 431–440 (1993).

Acknowledgements. We thank E. Ziff, G. Fishell, R. Brewster and C. Loomis for comments on the manuscript; K. Schulman for advice on selected tumour samples; L. Bernardo for cryostat sectioning; P. Censullo for help with tissue culture; E. Belloni and L. C. Tsui for a human *Shh* cDNA; E. Cordero for secretarial assistance; and J. Weider for help and advice with imaging. P.H. was a recipient of an Anne and Irving Holtzman fellowship in dermatopathology. This work was supported by a start-up grant from the Skirball Institute, a Basil O'Connor Award from the March of Dimes, and a fellowship from The Pew Scholars program in the biomedical sciences to A.R.A.

Correspondence and requests for materials should be addressed to A.R.A. (e-mail: ria@saturn.med.nyu.edu).

A SNARE involved in protein transport through the Golgi apparatus

Stephen Loucian Lowe, Frank Peter, V. Nathan Subramaniam, Siew Heng Wong & Wanjin Hong

Membrane Biology Laboratory, Institute of Molecular and Cell Biology, 15 Lower Kent Ridge Road, Singapore 119076, Singapore

In eukaryotic cells, the Golgi apparatus receives newly synthesized proteins from the endoplasmic reticulum (ER) and delivers them after covalent modification to their destination in the cell. These proteins move from the inside (*cis*) face to the plasma-membrane side (*trans*) of the Golgi, through a stack of cisternae, towards the *trans*-Golgi network (TGN), but very little is known about how proteins are moved through the Golgi compartments. In a model known as the maturation model[1–3], no special transport process was considered necessary, with protein movement along the Golgi being achieved by maturation of the cisternae. Alternatively, proteins could be transported by vesicles[4–6] or membrane tubules[7,8]. Although little is known about membrane-tubule-mediated transport[7,8], the molecular mechanism for vesicle-mediated transport is quite well understood, occurring through docking of SNAREs on the vesicle with those on the target membrane[4–6,9–13]. We have now identified a protein of relative molecular mass 27K which is associated with the Golgi apparatus. The cytoplasmic domain of this protein or antibodies raised against it quantitatively inhibit transport *in vitro* from the ER to the *trans*-Golgi/TGN, acting at a stage between the *cis*/medial- and the *trans*-Golgi/TGN. This protein, which behaves like a SNARE and has been named GS27 (for Golgi SNARE of 27K), is identical to membrin, a protein implicated earlier in ER-to-Golgi transport[14]. Our results suggest that protein movement from medial- to the *trans*-Golgi/TGN depends on SNARE-mediated vesicular transport.

Database searches using a *Caenorhabditis elegans* protein sequence (accession number P41941) that is weakly related to that of the yeast protein Bos1p, a v-SNARE involved in ER–Golgi transport[15–17], led to the identification of expressed-sequence tags (ESTs) encoding the potential human (accession number T88746) and mouse (accession numbers AA165867, W75416 and W30385) counterparts. Rat complementary DNAs were isolated by screening

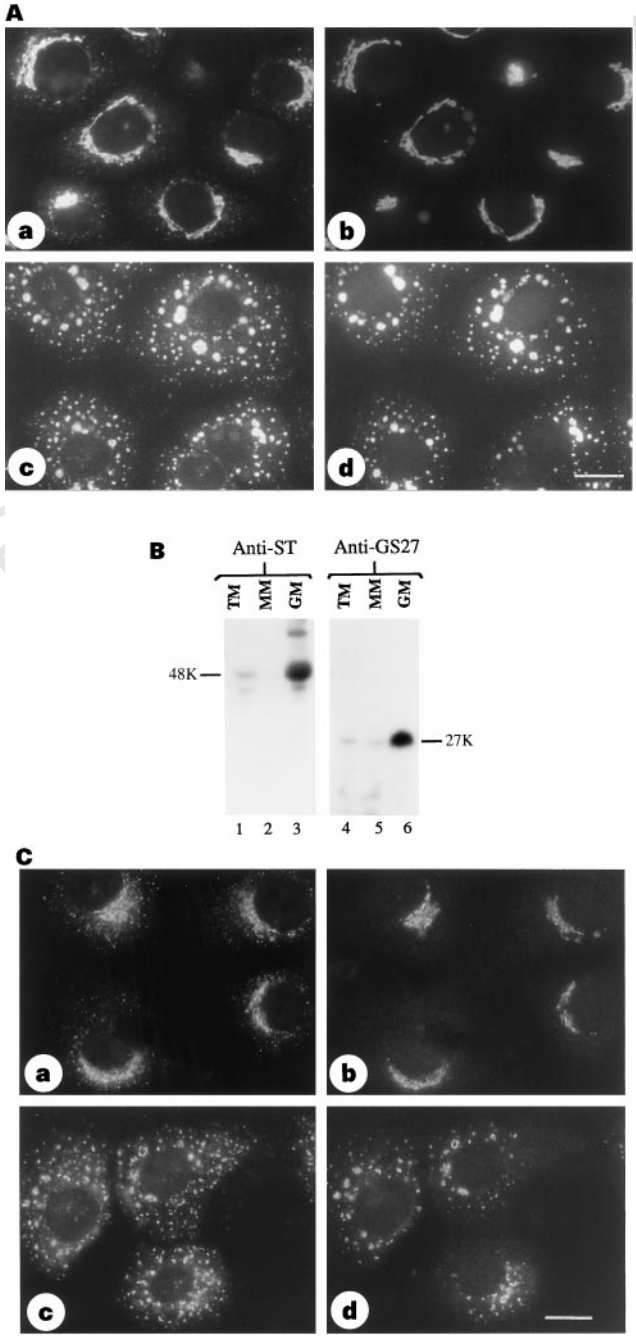

Figure 1 A, HA-epitope-tagged GS27/membrin is associated with the Golgi apparatus and vesicular structures. HA-GS27 (**a** and **c**) and Golgi mannosidase II (**b** and **d**) were double-labelled in control (**a**, **b**) and nocodazole-treated (**c**, **d**) cells. HA-GS27 was co-localized with mannosidase II in the control and in fragmented Golgi. The vesicular structures marked by GS27/membrin were devoid of mannosidase II labelling. **B**, Enrichment of GS27/membrin in the Golgi membrane. Proteins of total membranes (TM), microsomal membranes (MM) and Golgi-enriched membranes (GM) were analysed by immunoblot analysis using antibodies against α2, 6-sialyltransferase (ST) (lanes 1–3) or antibodies against GS27/membrin (lanes 4–6). **C**, Endogenous GS27/membrin is associated with the Golgi apparatus and its vesicular structures. Control (**a**, **b**) or nocodazole-treated (**c**, **d**) cells were double-labelled with antibodies against GS27/membrin (**a** and **c**) or Golgi mannosidase II (**b** and **d**).